



Research Paper

Microvascular networks in the area of the auditory peripheral nervous system



Han Jiang ^a, Xiaohan Wang ^b, Jinhui Zhang ^a, Allan Kachlmeier ^a, Ivan A. Lopez ^c, Xiaorui Shi ^{a,*}

^a Oregon Hearing Research Center, Department of Otolaryngology / Head & Neck Surgery, Oregon Health & Science University, Portland, OR, 97239, USA

^b Boston Children's Hospital, Harvard Medical School, 25 Shattuck Street, Boston, MA, 02115, USA

^c Cellular and Molecular Biology of the Inner Ear Laboratory, Department of Head and Neck Surgery, David Geffen School of Medicine at UCLA, LA, CA, 90095, USA

ARTICLE INFO

Article history:

Received 4 September 2018

Received in revised form

14 November 2018

Accepted 28 November 2018

Available online 4 December 2018

Keywords:

Mouse cochlea

Tissue clearing

Vascularity

Spiral limbus

Spiral ganglion neuron

ABSTRACT

Using transgenic fluorescent reporter mice in combination with an established tissue clearing method, we detail heretofore optically opaque regions of the spiral lamina and spiral limbus where the auditory peripheral nervous system is located and provide insight into changes in cochlear vascular density with ageing. We found a relatively dense and branched vascular network in young adults, but a less dense and thinned network in aged adults. Significant reduction in vascular density starts early at the age of 180 days in the region of the spiral limbus (SL) and continues into old age at 540 days. Loss of vascular volume in the region of spiral ganglion neurons (SGN) is delayed until the age of 540 days. In addition, we observed that two vascular accessory cells are closely associated with the microvascular system: perivascular resident macrophages and pericytes. Morphologically, perivascular resident macrophages undergo drastic changes from postnatal P7 to young adult (P30). In postnatal animals, most perivascular resident macrophages exhibit a spherical or nodular shape. In young adult mice, the majority of perivascular resident macrophages are elongated and display an orientation parallel to the vessels. In our imaging, some of the perivascular resident macrophages are caught in the act of transmigrating from the blood circulation. Pericytes also display morphological heterogeneity. In the P7 mice, pericytes are prominent on the capillary walls, relatively large and punctate, and less uniform. In contrast, pericytes in the P30 mice are relatively flat and uniform, and less densely distributed on the vascular network. With triple fluorescence labeling, we did not find obvious physical connection between the two systems, unlike neuronal-vascular coupling found in brain. However, using a fluorescent (FITC-conjugated dextran) tracer and the enzymatic tracer horseradish peroxidase (HRP), we observed robust neurovascular exchange, likely through transcytotic transport, evidenced by multiple vesicles present in the endothelial cells. Taken together, our data demonstrate the effectiveness of tissue-clearing methods as an aid in imaging the vascular architecture of the SL and SGNs in whole mounted mouse cochlear preparations. Structure is indicative of function. The finding of differences in vascular structure in postnatal and young adult mice may correspond with variation in hearing refinement after birth and indicate the status of functional activity. The decrease in capillary network density in the older animals may reflect the decreased energy demand from peripheral neural activity. The finding of active transcytotic transport from blood to neurons opens a potential therapeutic avenue for delivery of various growth factors and gene vectors into the inner ear to target SGNs.

© 2018 The Authors. Published by Elsevier B.V. This is an open access article under the CC BY-NC-ND license (<http://creativecommons.org/licenses/by-nc-nd/4.0/>).

1. Introduction

The inner ear is a high-energy demand organ. Microvascular

networks, critical for hearing, are situated in different locations of the cochlea. The major vascular networks are located in the cochlear lateral wall, receiving ~80% of cochlear blood flow (Gyo, 2013). The next largest vascular network is located in the region of the osseous spiral lamina, two plates of bone through which filaments of the acoustic nerve pass, and spiral modiolus, consolidating spiral ganglion neurons (SGNs), receiving ~19%–24% of

* Corresponding author.

E-mail address: shix@ohsu.edu (X. Shi).

blood flow, based on experiments in different species (Angelborg et al., 1984; Gyo, 2013; Nakashima et al., 2001). Although the volume of blood flow to the spiral limbus and SGN is lower than to the cochlear lateral wall, it is critical for neuronal activities. Constant sound stimulation to the inner ear imposes a high energy demand on neurons, requiring rapid delivery of oxygen and glucose.

Acoustic peripheral neurons and axons to hair cells are protected, forming enclaves in the solid bone of the spiral limbus and spiral lamina (Axelsson, 1988). The vascular system in this region is structurally complicated, and vascular physiology is largely unknown. Information on vascular pathophysiology in this region is limited by access into the bony region as well as by the anatomical tortuosity of the blood vessels. Conventional histology methods are not well suited for tracing this vascular network. In this study, we use transgenic fluorescent reporter mice in combination with a newly adopted “tissue clearing” method, reported early by MacDonald and Rubel (MacDonald and Rubel, 2008), to investigate the vascular system in this area and characterize its morphology in young adult and aged animals. We demonstrate the efficacy of the clearing method on vascular networks, comparing visualization in un-cleared and cleared tissue samples. We found the visualization of vascular architecture in the SL and SGN of whole mounted mouse preparations was markedly improved with the tissue-clearing approach. With the protocol, we also found vascular density in the region of the spiral limbus begins to fall at 180 days and continues to decline into old age. In addition, we identified two types of accessory cells, pericytes, and perivascular resident macrophages, which have close relationships with the blood vessels. Pericytes, vital for vascular integrity, fine regulation of the blood flow, and vascular permeability, densely populate vascular walls. In addition, a large population of resident macrophages are located around vascular networks. Both pericytes and perivascular resident macrophages undergo morphological transformations, displaying considerable heterogeneity in the course of development from postnatal to adulthood. Since structure always reflects function, the structural differences in vascular integration we see between postnatal and mature mice may reflect the stage of hearing development.

Neural activity requires a tightly controlled blood supply, including tight control over the transport of ions needed for synaptic transmission and other neural function (Andreone et al., 2015). How does the vascular system interact with the nervous system to meet this demand and sustain hearing activity? In this study, we used double or triple immunofluorescence labeling to investigate the structural interaction between the vascular and neural system. Although we found no direct structural contact, we did find communication. With fluorescence confocal and transmission electron microscopy, we identified strong indications of active neurovascular transport, observing the distribution of fluorescent tracers from blood and micro-particles released by pericytes in the SGNs. Although the mechanism of the transport pathway between blood and SGNs is not clear, the close inter-relationship between the microcirculation and the neural system may be essential for neural survival and activity under normal conditions. The inter-relationship also opens a potential therapeutic avenue for delivery of therapeutic agents, growth factors, or gene vectors into the inner ear to target SGN survival.

2. Materials and methods

2.1. Animals

C57BL/6J (Stock NO: 000664), Tg (Cspg4-DsRed.T1)1Akik/J (Stock No: 008241) and B6.129P-Cx3cr1^{tm1Litt}/J (Stock No: 005582) mice, originally purchased from Jackson Laboratory (Bar Harbor, ME, USA), were inbred and used at age postnatal day 7–180 days.

Aged C57BL/6J mice (360 days and 540 days) were directly purchased from the Jackson Laboratory aging service. The protocol for the care and use of these animals was approved by the Institutional Animal Care and Use Committee at Oregon Health & Science University (IACUC approval number IS00000968).

2.2. Vascular staining

Lectin-DyLight 649 (DL-1178, Vector Laboratories) and 40 KD FITC-Dextran (FD40S, Sigma) were diluted in 0.1 M PBS buffer to a concentration of 20 µg/ml and 10 mg/ml. Mice were anesthetized with ketamine hydrochloride (100 mg/kg, Intraperitoneal) and 2% xylazine hydrochloride (10 mg/kg, Abbott Laboratories, USA) and injected via the intravenous retro-orbital sinus with Lectin-DyLight 649 (0.1 ml per mice) and FITC-Dextran (2 mg/20g). After injection, the mice were placed on a water heated pad for 10 min until they were sacrificed for cochlear isolation.

2.3. Tissue clearance

The mice were sacrificed by cervical dislocation, and cochleae were isolated from different aged mice (30 days, 180 days, 360 days, and 540 days), and fixed in 4% paraformaldehyde (PFA) in 0.1 M sodium-potassium phosphate buffer (PBS), pH 7.4, overnight on a rocker at 4 °C. After decalcification in bone decalcifier (Decal Chemical Corporation, Tallman, NY, 1210) overnight on a rocker at 4 °C, the cochleae were micro-dissected to remove the lateral wall and cut into three pieces (apex, midbase, and base). The dissected specimens were decalcified for three more days by submerging the specimens in 10% ethylenediamine tetraacetic acid-disodium salt (EDTA) in PBS, pH 7.4, on a rocker at 4 °C. The specimens were rinsed free of EDTA 3 times with 10 min changes of PBS, and transferred to 70% ethanol, three times for 2 h. Dehydration continued with 95% ethanol for 30 min, followed by two changes of absolute ethanol for 2 h each. Five parts methyl salicylate (Sigma, M6752) were mixed with three parts benzyl benzoate (Sigma, B6630) for a clearing agent. The specimens were cleared in a 1:1 mixture of clearing agent and absolute ethanol overnight, followed by three changes of 100% clearing agent for 2 h and overnight, respectively. All clearing steps were carried out at room temperature with gentle agitation on a platform rotator. The cleared specimens were mounted in clearing agent and visualized under an FV1000 Olympus laser-scanning confocal microscope. The tissue was cleared with methyl salicylate and benzyl benzoate, named MBSS (MacDonald and Rubel, 2008).

2.4. Frozen sections and immunolabeling

Cochleae were isolated from vessel labeled C57BL/6J mice at different ages (7 days, 30 days, 180 days, and 360 days), and fixed in 4% PFA overnight. After decalcification at 4 °C overnight, the cochleae were dehydrated in 30% sucrose and embedded with OCT. Sections of the cochleae at 12 µm thickness were cut in the mid-modiolar plane. The crysolides were washed with PBS for 15 min to remove the OCT component, sections permeabilized in 0.5% Triton X-100 (Sigma Aldrich) for 30 min, and incubated in 10% normal goat serum and 1% BSA diluted in PBS for 1 h to block nonspecific binding sites. The sections were incubated overnight with primary antibody anti-beta III tubulin (801201, Biolegend, 1:200) at 4 °C. The sections were subsequently stained with an appropriate fluorescence-conjugated secondary antibody, either Alexa Fluor 488-AffiniPure Goat Anti-Mouse IgG, Fc Subclass 2a (115545206, Jackson immuno research lab, 1:200) or Alexa Fluor 568-conjugated goat anti-rabbit IgG, at 37 °C for 1 h. The tissues were washed for 30 min, mounted (H-1000, Vector Laboratories,

USA), sealed in 20% glycerol, and visualized under an FV1000 Olympus laser-scanning confocal microscope. Controls were prepared by replacing primary antibodies with overnight incubation in 1% BSA-PBS.

2.5. Whole mount preparation of P30 mouse cochlea

To demonstrate the morphology of pericytes and resident macrophages in the young adult (30 days) mouse cochlea, we used fluorescent reporter Tg (Cspg4-DsRed.T1)1Akik/J mice, in which all NG2 positive pericytes are fluorescent labeled, and B6.129P-Cx3cr1tm1Litt/J mice, in which all macrophages are fluorescent labeled. The mice were injected with a fluorescent dye. The blood vessels were labeled with lectin-DyLight 649 (Cat. No: DL-1178, Vector Lab.). The animals were then sacrificed, and the cochleae isolated and fixed in 4% PFA overnight. The next day, the tissue samples were isolated and the region of spiral ganglion neurons exposed after gently breaking the covering bone and removing the chips surrounding the spiral ganglion. The tissue samples were examined and recorded under an FV1000 Olympus laser-scanning confocal microscope. This simple “gentle-bone-breaking” preparation enables us to preserve the fluorescence signal from pericytes and macrophages (in contrast, the fluorescence signal is attenuated when the tissue is decalcified and MBSS cleared).

2.6. Measurement of capillary density

Morphometric measurements of the vascular networks were obtained in two areas: the region of spiral ganglion neurons (SGNs) and the region of the spiral limbus (SL). SGNs were labeled with anti- β -III tubulin to distinguish the SGN and SL region. Blood vessels were labeled with the fluorescent dye lectin-DyLight 649. Regions of SGN and SL at each cochlear turn were manually traced from the channel uniquely displaying SGN and SL labeling in the confocal image. The pixel area of the SGN and SL was assessed with Image J (NIH, 1.51t). In addition, the pixel area of the vasculature in each region of interest at each cochlear turn was also determined using Image J (NIH, 1.51t). The channel uniquely showing vessels was separated from the confocal image, and the threshold adjusted to maximize vessel intensity relative to background. If the vessel had weak fluorescent labeling (the fluorescence signal below a pre-set threshold), but the vessel contour (border) could still be visualized by eye, the vessels were traced manually in zoomed-in images to obtain the maximum possible accuracy. The vascular density was assessed as a percentage of vascular pixel area/pixel area of SGN or SL in each measured area and at each turn. The data were averaged as mean \pm SEM determined from 4 or 6 whole mounted specimens.

2.7. Transmission electron microscopy (TEM)

The cochleae were isolated and perfused with a fixative of 3% glutaraldehyde and 1.5% PFA overnight. Strial tissues were then removed and post-fixed in 1% osmium (Electron Microscopy Sciences, Hatfield, PA). Tissues were dehydrated through a graded alcohol series and embedded in Embed 812 (Electron Microscopy Sciences, Hatfield, PA), sectioned, stained with lead citrate (Electron Microscopy Sciences, Hatfield, PA) and uranyl acetate (Electron Microscopy Sciences, Hatfield, PA), and viewed on a Philips CM 100 transmission electron microscope (Philips/FEI Corporation, Eindhoven, Holland). For determination of how horseradish peroxidase (HRP) tracer is distributed in the region of SGNs, Type II HRP (P8250, Sigma-Aldrich, USA) solution at 100 μ l (50 mg/ml) was intravenously administered to animals. 30 min later, heart perfusion was performed with 1 \times PBS (pH 7.4) to flush the circulating

blood. Cochleae were isolated and fixed with phosphate-buffered 3% glutaraldehyde and 1.5% PFA for 5 h. The stria vascularis was isolated and incubated in reaction buffer (Pierce™ DAB Substrate Kit, 34002, Thermo Fisher Scientific, USA) containing DAB and stable peroxide substrate for 1 h. After the chemical reaction, samples were post-fixed for 1 h in 1% osmium. Tissues were dehydrated through a graded alcohol series, embedded in Embed 812 (Electron Microscopy Sciences, Hatfield, PA, USA), sectioned, stained for 2 min with UranyLess (Electron Microscopy Sciences, USA), and examined on a transmission electron microscope (FEI Tecnai T12 TEM-120KV, Hillsboro, Oregon USA).

2.8. Statistics

Data were presented as means \pm SEM. GraphPad Prism 6.0 software was used for the statistical analysis. Data were compared using one-way ANOVA followed by a Turkey multiple comparison. $P < 0.05$ was considered statistically significant.

3. Results

3.1. Visualization of integrated vascular architecture in the region of the spiral limbus and spiral ganglion neurons is much ‘refined’ with the tissue-clearing approach

Microvascular networks in the region of the SL and SGN comprise various size blood vessels, providing around 19%–24% blood supply to the peripheral auditory nerve system, including SGNs and its peripheral nerve processes (Angelborg et al., 1984; Nakashima et al., 2001). The visualization of large-scale volumetric models of vascular structure in this region is often difficult and limited by the optical scattering and absorption of light by bone. In this study, using a clearing MSBB mixture on the bony samples, the optical aberration in the cochlear specimens is greatly reduced in adult mouse cochlea. In particular, using this method in combination with injection of a fluorescence indicator, Lectin-DyLight 649, for labeling blood vessels, the full volume of the vasculature is clearly obtained under laser scanning confocal microscopy. Fig. 1 is a representative confocal fluorescence projection image from a C57BL/6 mouse demonstrating the dramatic improvement in visualization of vessel networks before (A) and after (B) MSBB clearing. Compared to conventional fluorescence labeling without tissue-clearing, we found that details of vascular architecture in the spiral limbus and SGN in whole mounted mouse preparations is markedly enhanced. This procedure enables large-volume imaging of the vascular structure, including the large vessels and smaller (and rarer) blood vessels, over long distances.

3.2. Demonstration of integrated vascular architecture in different regions and turns of young adult mice

The MBSS method, in combination with a standard method of immunofluorescence labeling for SGNs, enables simultaneous identification of vascular beds in different regions at different cochlear turns. Fig. 2(A–C) is a representative cleared sample from adult (P30 days) C57BL/6 mouse cochlea. With immunofluorescence labeling for β -III tubulin antibody, a marker for SGNs, we can segment the vascular beds in different regions, including regions of the SL and SGN. Consistent with the vascular structure seen in humans (Axelsson, 1988), blood vessels in the spiral modulus (SM) form “vascular spring-coils” which run through the bony parts of the modiolus to the osseous SL. Vessels in the SL and SGN are straighter, irregular and branched, providing the main blood supply to SGNs and its peripheral nerve processes. With image processing, the vascular structure in the different regions and turns can be

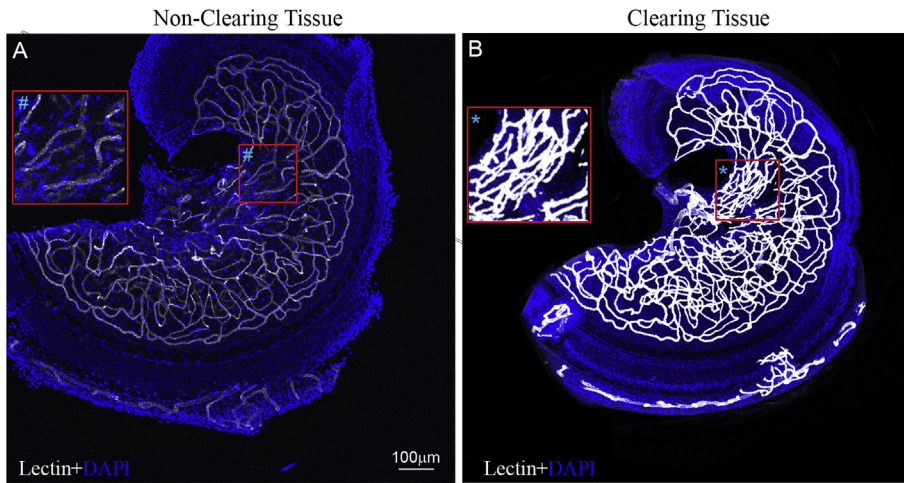


Fig. 1. Visualization of vessels in the region of the SL and SGN is markedly improved with MSBB clearing. (A) A confocal fluorescence projection image shows decalcified cochlear tissue from the apex of a C57BL mouse at 30 days without MSBB clearing. (B) A confocal fluorescence projection image shows the same specimen after clearing with MSBB. Visualization of the vessels is improved. Mice were injected with lectin-DyLight 649 (white) to label vessels. Tissues were stained with DAPI for cell nuclei. (#) and (*) in panels A and B are selected areas highlighting the difference in visualization of the vascular networks between the two preparations.

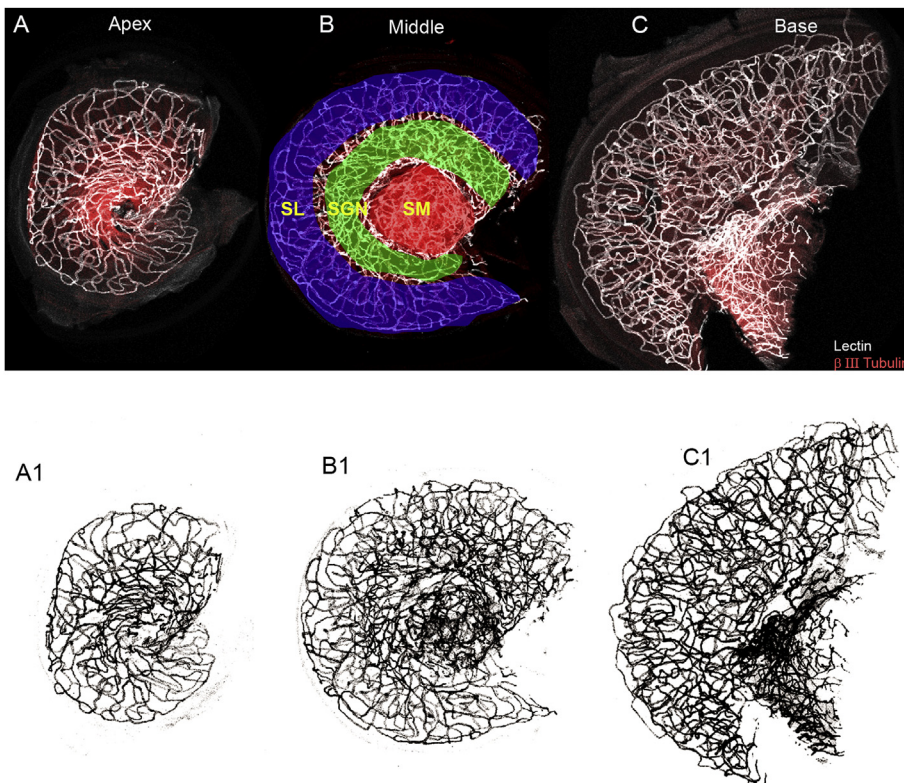


Fig. 2. Demonstration of vascular networks in different regions at different turns in a C57BL mouse cochlea. (A–C) Confocal images of MSBB cleared cochlear tissues at different turns – apex, midbase, and base. SGNs and peripheral nerve fibers were labeled with anti- β -III Tubulin for distinguishing vascular networks situated in different anatomic regions. (A1)–(C1) are selected lectin labeled channels to demonstrate vascular networks at the different turns – spiral modular, spiral limbus (SL), and spiral ganglion neuron (SGN) are clearly visualized. SL: spiral limbus; SGN: Spiral ganglion neuron; SM: Spiral modulus.

parsed apart by selecting a vascular labeling channel, as demonstrated in Fig. 2A1–C1. Vascular volume at those locations of the different turns can also be measured and compared.

3.3. Reduction in capillary density with aging parallels loss of spiral ganglion neurons

Loss of blood vessels in the cochlear lateral wall is known to

contribute to the pathology in aging-related and other forms of sensorineural hearing loss (Neng et al., 2015; Shi, 2016). However, very little vascular information has been collected in the area of the spiral limbus and SGNs. In this study, using the established MBSS tissue clearing approach, we examined changes of vascular density in the two regions of the mouse cochlea over a range of animal age: 30 days, 180 days, 360 days, and 540 days. Fig. 3A–D are vascular networks from different turns. Our data showed that vascular

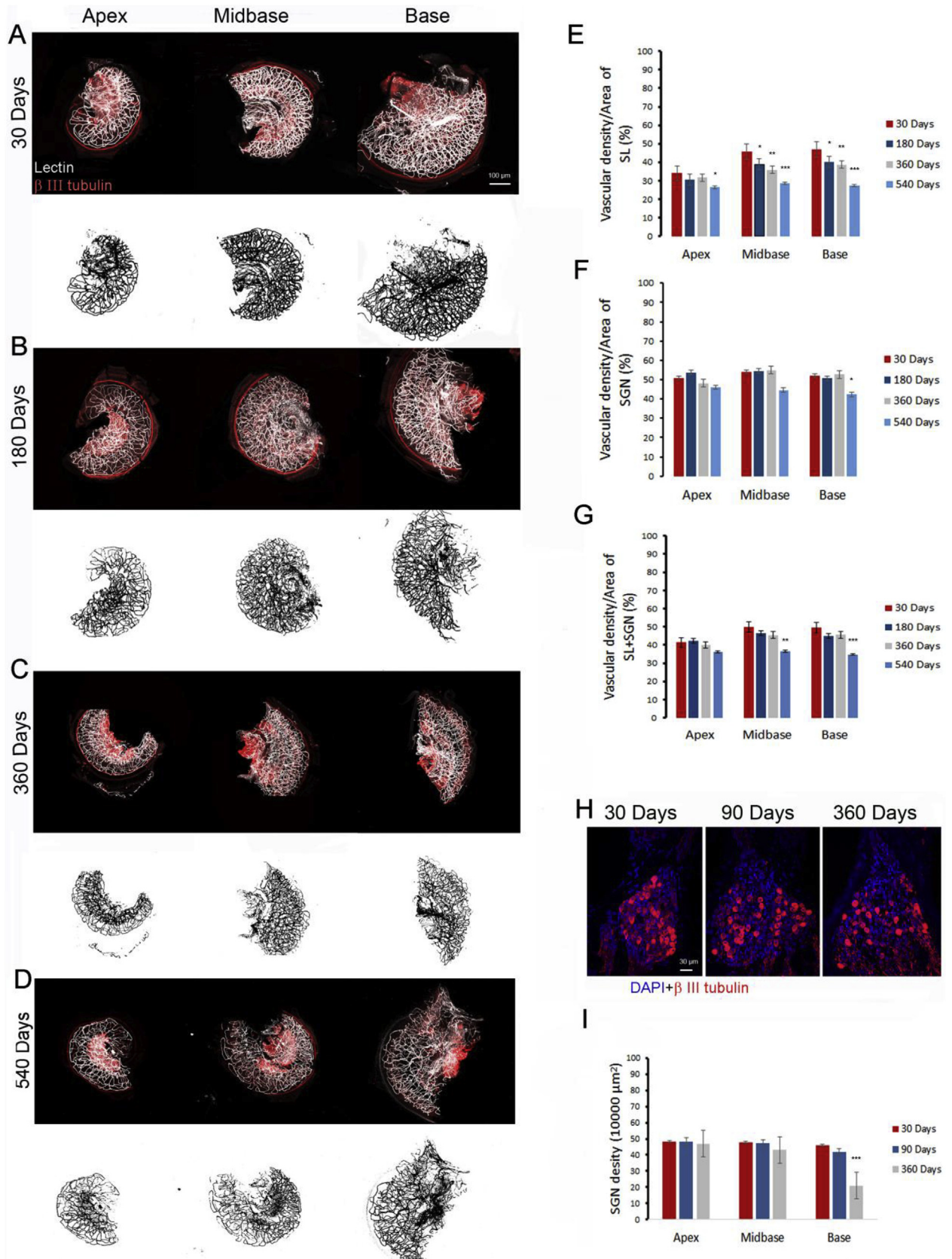


Fig. 3. Reduction in capillary density with aging parallels loss of spiral ganglion neurons. (A–D) Confocal images of MSBB cleared cochlear tissue at different turns (apex, midbase, and base) at different ages. Vessels were labeled by a lectin injected into the retro-orbital vein. Spiral ganglion neurons were immuno-labeled with β -III tubulin. (E–G) Vascular density measured in regions of the SL and SGNs from different turns at different ages ($n = 6$ for group 30 days, 180 days, and 360 days, $n = 4$ for group 540 days). (E) In the SL region, significant differences are found at 540 days compared to at 30 days for the apex [${}^{***}\mathbf{P}_{\text{apex}}(540 \text{ vs } 30) = 0.024$, $\mathbf{F}_{\text{apex}}(3,21) = 3.848$]. Significant differences are found at 180 days, 360 days, and 540 days compared to at 30 days for the midbase [${}^{***}\mathbf{P}_{\text{midbase}}(180 \text{ vs } 30) < 0.001$; $\mathbf{F}_{\text{midbase}}(3,21) = 13.68$]. Significant differences are found at 180 days, 360 days, and 540 days compared to at 30 days for the base [${}^{***}\mathbf{P}_{\text{base}}(180 \text{ vs } 30) < 0.001$; $\mathbf{F}_{\text{base}}(3,21) = 19.29$]. (F) In the SGN region, significant difference are found at 540 days compared to at 30 days for the base [${}^{***}\mathbf{P}_{\text{base}}(540 \text{ vs } 30) = 0.028$, $\mathbf{F}_{\text{base}}(3,21) = 3.632$]. (G) In the SL and SGN region, significant differences are found at 540 days compared to at 30 days for the midbase [${}^{**}\mathbf{P}_{\text{midbase}}(540 \text{ vs } 30) < 0.01$, $\mathbf{F}_{\text{midbase}}(3,46) = 3.549$] and base [${}^{**}\mathbf{P}_{\text{base}}(540 \text{ vs } 30) < 0.001$, $\mathbf{F}_{\text{base}}(3,50) = 7.584$]. (H) Confocal images of SGNs at different ages. (I) Significant differences are found at 360 days compared to at 30 days for the base [$n = 6$ for each age, ${}^{***}\mathbf{P}_{\text{base}}(360 \text{ vs } 30) < 0.001$; $\mathbf{F}_{\text{base}}(2,11) = 22.97$]. * $P < 0.05$, ** $P < 0.01$, *** $P < 0.001$.

volume is gradually reduced with aging. In particular, the density of the capillary network in the region of the SL starts to decline as early as 180 days in the middle-base turns, and continues to decline further with aging. However, the reduction of vascular volume in the region of SGNs only declined at the basal turn at a much older age (540 days). Fig. 3E–G are assessments of vascular volume in the regions of the SL and SGNs and together (*P < 0.05, **P < 0.01, ***P < 0.001, n = 6 for group 30 days, 180 days, and 360 days, n = 4 for group 540 days). In this study, we also assessed density of SGNs at different ages (n = 6). Consistent with reports from other labs (Bao and Ohlemiller, 2010; Kujawa and Liberman, 2015), we found aged animals showed loss of SGNs. Fig. 3H shows progressive decline in SGN density in the lower base of 360 day old mice. The packing density of SGNs in Rosenthal's canal appeared highest in the modiolus of the young adult. Neuron density was much lower in the base of 360 day old mice. A graph of this age-related effect on SGN density is shown in Fig. 3I. Taken as a whole, our data shows parallel loss of capillary volume and SGNs in aged animals. However, it remains to be determined whether loss in capillary volume and SGN density is correlated.

3.4. The vascular system in the spiral limbus and SGNs contains two major types of accessory cells – tissue resident macrophages and pericytes

3.4.1. Tissue resident macrophages surround blood vessels and have a close relationship with vascular networks

Presence of tissue resident macrophages in the acoustic peripheral nervous system has previously been demonstrated (Bas et al., 2015; Kaur et al., 2015; Okano et al., 2008). However, the relationship between tissue resident macrophages and the vascular system has not been heretofore investigated. In this study, we demonstrate the structural interaction between the macrophages and vascular system using fluorescent reporter CX3CR1-GFP mice (macrophages GFP-labeled green). Vessels were stained with a fluorescent lectin dye administered through retro-orbital injection. We found tissue resident macrophages surrounding blood vessels, some caught in the act of transmigrating from the circulation in cross-sections of the tissue (Fig. 4A–C). We also found the macrophages undergo drastic changes in morphology from P7 to young adult (P30). Fig. 4A–C are representative confocal projection images showing the morphology and distribution of resident macrophages enshrouding vessels at P7. Notably, the resident macrophages at P7 exhibit a spherical or nodular shape, in contrast to an elongated shape and orientation parallel to vessels in the adult, as shown in Fig. 4D–J. The differences in morphology seen in postnatal and young adults might reflect the state of maturation and existence of functions related to adaptive immune response. The macrophages surrounding vascular walls might serve as progenitor cells for postnatal vasculogenesis or contribute to repair of damaged vessels as part of the local inflammatory response.

3.4.2. Pericytes densely populate vascular networks and display heterogeneity

Pericytes are another type of vascular accessory cell, widely distributed on micro-vessels in the body (Shi, 2016; Shi et al., 2008). Anatomically, the pericytes are embedded in the vascular basement membrane of endothelial cells, contributing to the integrity of blood vessels (Neng et al., 2013). Pericytes are known to display a heterogeneous range of morphology, phenotype, and function in different tissues (Dias Moura Prazeres et al., 2017). In this study, we used an NG2DsRedBAC transgenic mouse in which pericytes express an optimized red fluorescent protein variant (DsRed.T1) under the control of an NG2 (Cspg4) promoter. All NG2 positive cochlear pericytes in this model are fluorescent labeled. We found

that vascular networks in the SGNs and peripheral processes are densely populated by pericytes, analogous to pericyte distribution in the stria vascularis. Pericytes in early postnatal and young adults are morphologically similar, but we noticed slight differences on close examination. The majority of pericytes in postnatal P7 animals have a prominent nucleus and cytoplasmic puncta, and are tightly associated with the abluminal surface of the endothelium. In young adult 30 day old animals, pericytes are flatter and more evenly distributed on the capillaries. Fig. 5 compares representative confocal images of pericytes on vascular networks in the mouse cochlea at P7 (A1–A4) and P30 (B1–B4). The difference in cellular structure may parallel auditory function, as pericytes are critical for blood flow regulation and maintaining vascular stability.

3.5. Structural connections between the vascular and neural system

What is the relationship between the vascular and neural system in the SGN? To investigate the structural links between the vascular and neural system, we used a double transgenic fluorescent reporter mouse in combination with immunofluorescent labeling. Cross sections (Fig. 6A–D) and whole mounts (Fig. 6E–G) show blood vessels ‘intertwining’ and “winding” the neurons. There appears to be physical contact between the vascular and neural system. However, anatomical connections cannot be clearly distinguished under confocal fluorescence microscopy. To investigate the presence or absence of structurally interactive architecture, and characterize different cells in the vascular and neural system, we employed TEM to obtain details at the ultrastructural level. We found, unlike neural-vascular coupling in the brain, vessels in this region of the cochlea are not directly connected with neurons and acoustic nerve fibers (Fig. 6H–J).

3.6. Cross-talk between the blood circulation and SGNs

In this study, we found, based on a few observations, the presence of communication via trans-endothelial transport between SGNs and blood vessels. When we intravenously injected animals with a lectin (labeling blood vessels) and a 40 kD FITC-dextran tracer, the tracer or lectin was transported from blood vessels to the extracellular space, but both were quickly (within 10 min) taken up by SGNs, as shown in Fig. 7A–C. Second, in NG2+ pericyte fluorescent reporter mice, we observed NG2-positive particles (likely released by pericytes) in the cytoplasm of SGNs (Fig. 7D–F). The events are clearly visualized in magnified images, see Fig. 7G–I. These phenomena are suggestive of active communication between the vascular and neural system. To further verify the active communication we used HRP, an enzymatic tracer, in conjunction with transmission electron microscopy (TEM), to trace the path of the transport at the ultrastructural level. We found multiple HRP containing vesicles in endothelial cells, as shown in Fig. 7J–L. HRP signal is seen in the soma of endothelial cells and SGN membranes 30 min after HRP was administrated in the blood stream. The communication between the circulatory system and neurons suggests transcytotic transport from blood to neurons may be the essential conveyance for nutrients, ions, and growth factors from the blood stream to SGNs.

4. Discussion

Visualization of the vasculature in the spiral ganglion and peripheral processes is markedly improved with the MSBB clearing protocol. With this approach, we also found progressive decline in capillary density in the spiral limbus and SGNs with aging, as well as accompanying loss of spiral ganglion neurons. Furthermore, we demonstrate two types of vascular accessory cells, resident

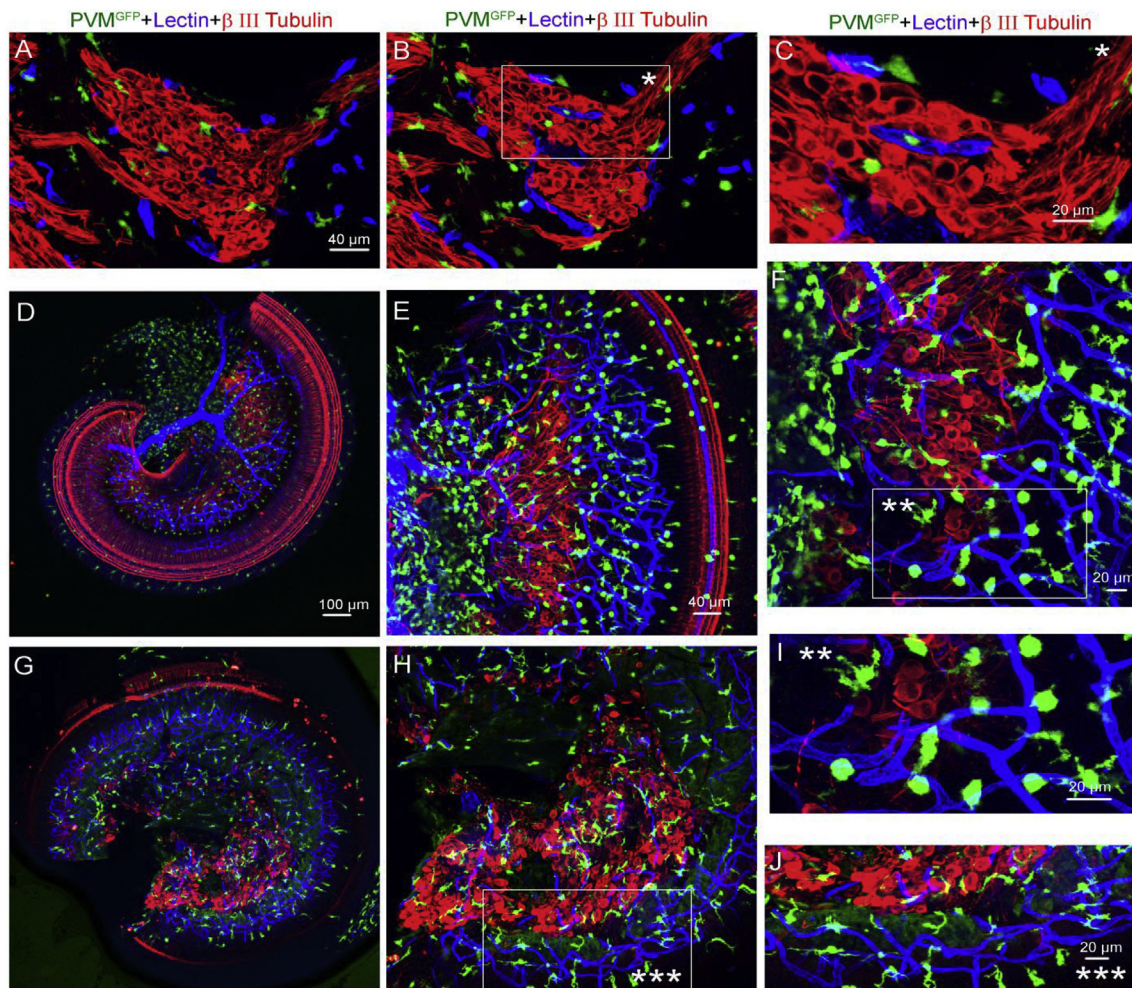


Fig. 4. Tissue resident macrophages enveloping blood vessels undergo drastic changes in morphology from P7 to P30. Cross-section of a cochlear spiral ganglion (A–C). Whole mounted cochlear preparation at P7 (D–F) and P30 (G and H) in CX3CR1-GFP mice. Macrophages were GFP-labeled (green), spiral ganglion neurons labeled with β -III Tubulin (red), and vessels with lectin. Macrophages at P7 exhibit a spherical or nodular shape (D–F). However, macrophages at P30 are elongated and display an orientation parallel to vessels (G and H). Panel I (**) from Panel F and Panel J (***) from Panel H are close-up images respectively showing the difference in morphology of pericytes and resident macrophages. PVM: perivascular resident macrophage. (For interpretation of the references to colour in this figure legend, the reader is referred to the Web version of this article.)

macrophages and pericytes, are associated with the vascular system. Tissue resident macrophages are located around vascular networks and undergo dramatic changes in morphology from postnatal animal to young adult. Pericytes, densely populating the vascular network, are also shown to display considerable morphological heterogeneity from postnatal animal to young adult. In the study, we used fluorescent labeling in combination with TEM to investigate intercellular contacts between the vascular and neural system. Although our TEM results show no evidence of direct contact between the two systems, we did detect signal communication between the vascular cells and neurons with fluorescent- and HPR-tracers. In particular, we found evidence that HRP accumulates in adjoining extracellular spaces and endothelial cell vesicles, suggestive of a transcytotic path in vascular-neuronal communication. The presence of multiple vesicles in endothelium could be a strong indicator of endocytotic transport between vessels and extracellular space. The endocytotic transport may be an essential conveyance for nutrients, ions, and growth factors from the blood stream to neurons in lieu of other mechanisms. Since structure is indicative of function, changes in vascular structure between postnatal and mature mice suggest parallel changes in functional integration. Progressive loss of vascular density, accompanied by loss in neurons, marks the progressive

degeneration in cochlear cells with aging.

4.1. The vascular architecture (vascular tree) is pruned with aging

Acoustic peripheral neurons and axons to hair cells are protected, forming enclaves in the solid bone of the spiral limbus and spiral lamina (Axelsson, 1988). The vascular system in this region is structurally complicated, and some of its physiology is unclear. Information on this region is sparse, limited by access into the bony region. Bony tissues are generally opaque, with scatter and absorption of light limiting resolution and optical depth. New tissue clearing techniques, however, enable researchers to visualize opaque organs and tissues in three-dimensional depth. In this study, we adopted a tissue clearing method reported on early by MacDonald and Rubel (MacDonald and Rubel, 2008) to obtain a global view of the vascular architecture.

Tissue-clearing methods are either aqueous reagent-based or organic solvent-based (Richardson and Lichtman, 2015). Aqueous reagent-based methods have a lower refractive index and are generally more suitable for use with remaining green fluorescent protein (GFP) or GFP-like fluorescent proteins (Jing et al., 2018). In contrast, organic solvent-based approaches, using a clearing medium with a high refractive index, enable the researcher to obtain

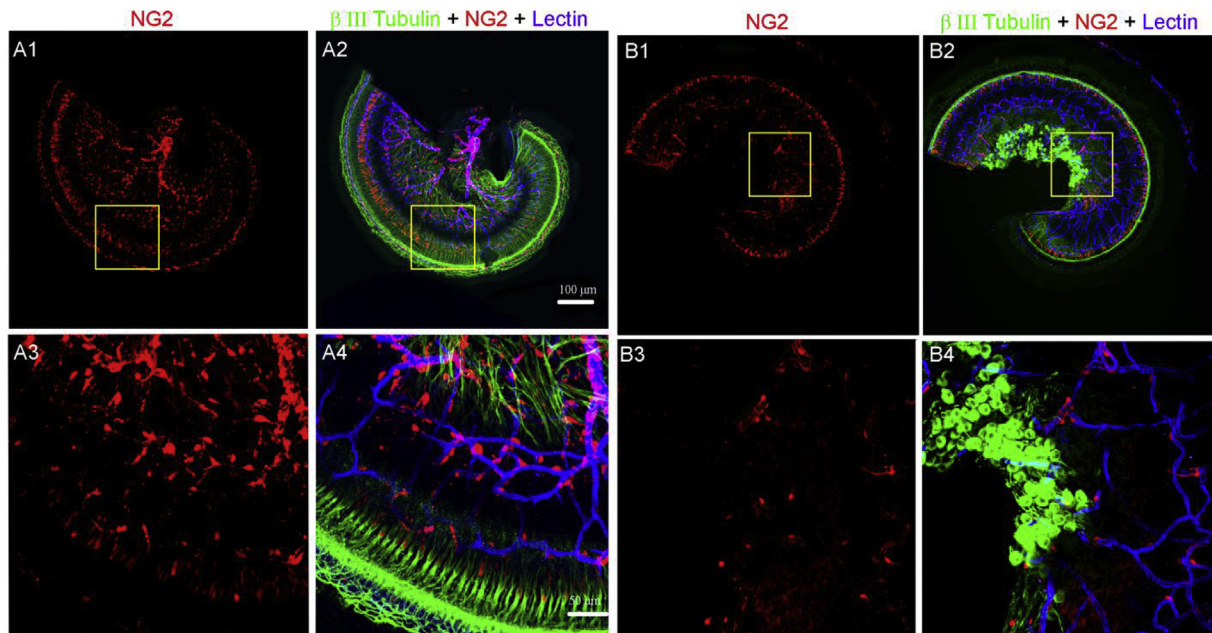


Fig. 5. Pericyte distribution on vascular networks in NG2DsRedBAC transgenic mouse cochleae at P7 and P30. (A1–B4) Confocal projection images in a whole mount preparation of cochlear tissue from apical turns at age P7 under low (A1–A2) and high magnification (A3–A4). Pericytes (red) densely populate blood vessels in the spiral ganglion and peripheral processes. Spiral ganglion neurons were labeled with β -III tubulin (green) and blood vessels with lectin. A relatively low density of pericytes is seen on the vascular networks in P30 mice, shown under low magnification (B1–B2) and high magnification (B3–B4). (For interpretation of the references to colour in this figure legend, the reader is referred to the Web version of this article.)

high tissue optical transparency. The clearing medium transforms intact tissue into a nanoporous hydrogel-hybridized form, allowing fine structural analysis of bony samples (Chung et al., 2013). In this study, we used an organic solvent-based method to clear a whole mount preparation of the osseous spiral limbus in combination with infusion to the circulation of a fluorescent lectin dye. Visualization of the full volume of the vasculature in the area is dramatically improved (as shown in Fig. 1). With an immunofluorescence label for acoustic neurons, we are also able to identify where capillaries arise from the main cochlear artery and start to form loops at the junction between the SL and SGN. Using morphometric measurements, we determined that vascular density starts to fall in the region of the SL at age 180 days at the middle-base turn in a C57BL mouse and continues to decline with aging. Significant vascular degeneration in the region of SGN is seen at the basal turn at the age of 540 days.

The microcirculation in the SL is based on rich capillary beds which participate in the transport of oxygen to the perilymph (Firbas et al., 1981) and provide nutrients to peripheral acoustic nerve fibers. In contrast, the vasculature in the SGN comprise terminal arterioles, capillaries, and veins (Axelsson, 1988). The large vessels such as arterioles and veins have thick, and resilient endothelial walls. Studies have shown that small vessels are more vulnerable to pathological conditions (Ostergaard et al., 2016). Small vessel pathology is a major contributor to brain stroke in the elderly (De Silva and Miller, 2016). The vascular degeneration identified in the region of the SL could be due to differences in the physical properties of the vessels and their functional vulnerability.

Paralleling the degeneration in vasculature with aging, the number of SGNs is also significantly reduced in aged animals. We found that SGNs are reduced by ~50% in 360 day old mice. However, it isn't known whether the loss in SGNs correlates with reduced vascular density. Normal micro-vessels are key to normal tissue and organ function (Ellis et al., 2005). Continuous cerebral blood flow is vital for neuronal survival. Recent research particularly highlights a

high degree of interplay between loss of neurons and vascular damage or degeneration (Kisler et al., 2017; Venkat et al., 2016). Chronic hypo-perfusion often produces cochlear hypoxia, which if the blood flow is not quickly restored, significantly accelerates deterioration of organ function. Although it is unknown whether loss in SGNs correlates with reduced capillary density, vascular degeneration related chronic hypoxia could be one of factors in acceleration of neural degeneration. It has been reported that neural degeneration is frequently accompanied by vascular regression in response to changes in brain metabolic activity (Noonan et al., 2015; Wilhelm et al., 2016). The loss of SGNs in the cochlea preceding loss of vascular volume could be a sign of decreased neural activity in the aged cochlea.

4.2. Vascular component cells: tissue resident macrophages and pericytes – their potential function

The presence of tissue resident macrophages in the acoustic peripheral nervous system was earlier reported (Bas et al., 2015; Dong et al., 2018; Kaur et al., 2015; Okano et al., 2008; Yagihashi et al., 2005). In this study, we show further relationships between tissue resident macrophages and blood vessels. We found that some of the macrophages are in circulation, as shown in Fig. 4. This suggests recruitment from blood-borne monocytes. We also found the macrophages to undergo morphological change from postnatal animal to young adult. In the postnatal mice, the macrophages are spherical or nodular in shape. By contrast, in adult animals, most tissue macrophages are elongated and oriented parallel to vessels. Cell shape is associated with cell function (Folkman and Moscona, 1978). For example, a recent study demonstrated macrophage function strongly dependent on size and shape (Doshi and Mitragotri, 2010). The morphological changes from postnatal animal to adult in tissue resident macrophages may reflect functional status related to surrounding environmental cues. A recent study by LN Brown (Brown et al., 2017) demonstrated macrophages in the

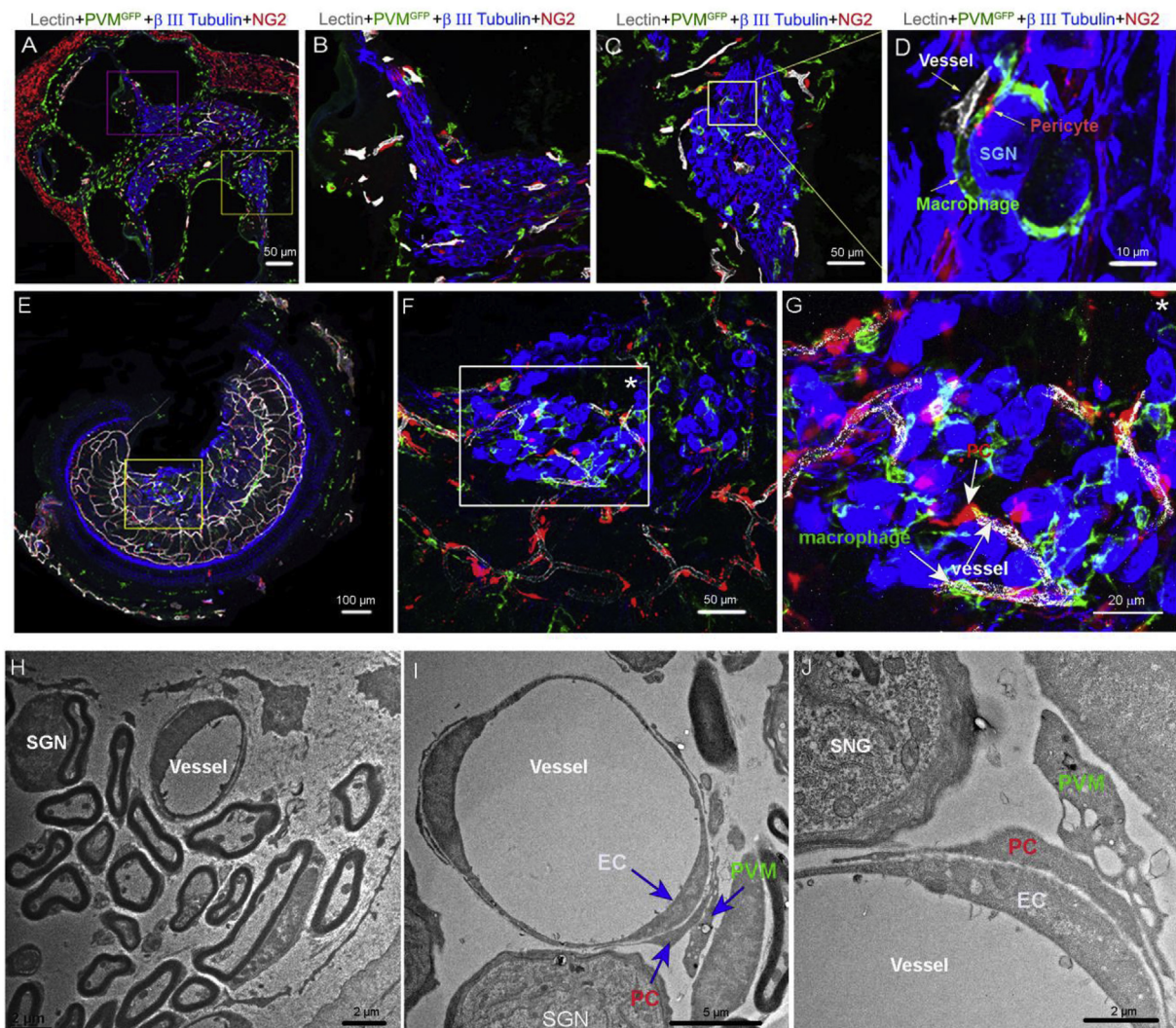


Fig. 6. Ultrastructural examination shows the capillaries are not connected to the spiral ganglion neurons. (A–C) Confocal projection cross section of a P7 NG2DsRedBAC/CX3CR1-GFP transgenic mouse cochlea, showing the vascular system interacting with the spiral ganglion. Pericytes were NG2-DsRed-labeled (red), PVMs GFP labeled (green), spiral ganglion neurons β-III Tubulin labeled (blue), and vessels stained with lectin (white). (D) is a close-up image from a region in panel C which shows cellular interactions between vascular endothelial cells, neurons, pericytes, and tissue resident macrophages. (E–G) Confocal projection of a whole mount preparation showing blood vessels 'intertwining' and "winding" the neurons and interacting with the spiral ganglion under low magnification (E) and high magnification (F and G). (H–J) TEM graphs show capillaries clearly separated from neurons, showing no physical contacts between them. SGN: Spiral ganglion neuron; PC: pericytes; PVM: perivascular resident macrophage; EC: endothelial cell. (For interpretation of the references to colour in this figure legend, the reader is referred to the Web version of this article.)

region of the spiral ganglion contribute to regulation of glial cell density and maturation of the postnatal auditory nerve in postnatal day 7 mice. The existence of branched macrophages in adulthood might be part of a local inflammatory response, as resident macrophages play a critical role in surveillance, scavenging, and tissue repair in the cochlea (Mitrasinovic and Murphy, 2002, 2005; Nimmerjahn et al., 2005). The resident macrophages scavenge invading microorganisms and dead cells, while acting as immune or immuno-effector cells, and produce superoxide anions, nitric oxide, and inflammatory cytokines during inflammation (Block and Hong, 2005, 2007; Cheret et al., 2008; Hanisch and Kettenmann, 2007). Studies from T Kaur (Kaur et al., 2015, 2018) have shown macrophages involved in inflammation-mediated acoustic neuronal loss following hearing loss from ototoxic or acoustic injury. Resident macrophages surrounding the vascular wall in this study indicate the macrophages might also serve as progenitor cells for postnatal vasculogenesis (Shapouri-Moghaddam et al., 2018; Vacca and Ribatti, 2011), contributing to repair of the damaged

vessels in local inflammatory response, as reported in other organs (Pacilli and Pasquinelli, 2009; Zengin et al., 2006).

Capillaries in the region are also richly populated by pericytes. The pericytes are distributed in a region and tissue-specific manner, with the density reflecting the specific function of the micro-vessel, tightly coupled to metabolic demand (Aguilera and Brekken, 2014; Hirschi and D'Amore, 1996; Sims, 2000). The function of pericytes in the microvascular networks in the region of the cochlear peripheral nervous system is unknown, however many studies have shown pericytes have a critical role in maintaining vascular stability and integrity, angiogenesis, and regulation of capillary blood flow in different organs (Armulik et al., 2010; Daneman et al., 2010; Hellstrom et al., 1999; Lindahl et al., 1998; Peppiatt et al., 2006; Wang et al., 2014). Pericyte-endothelial cell crosstalk is particularly known to promote the formation of endothelial tight junctions (Daneman et al., 2010). Pericyte deficiency related blood barrier breakdown has been seen in the blood-brain barrier (BBB), (Armulik et al., 2010; Crawford et al., 2013; Daneman et al., 2010;

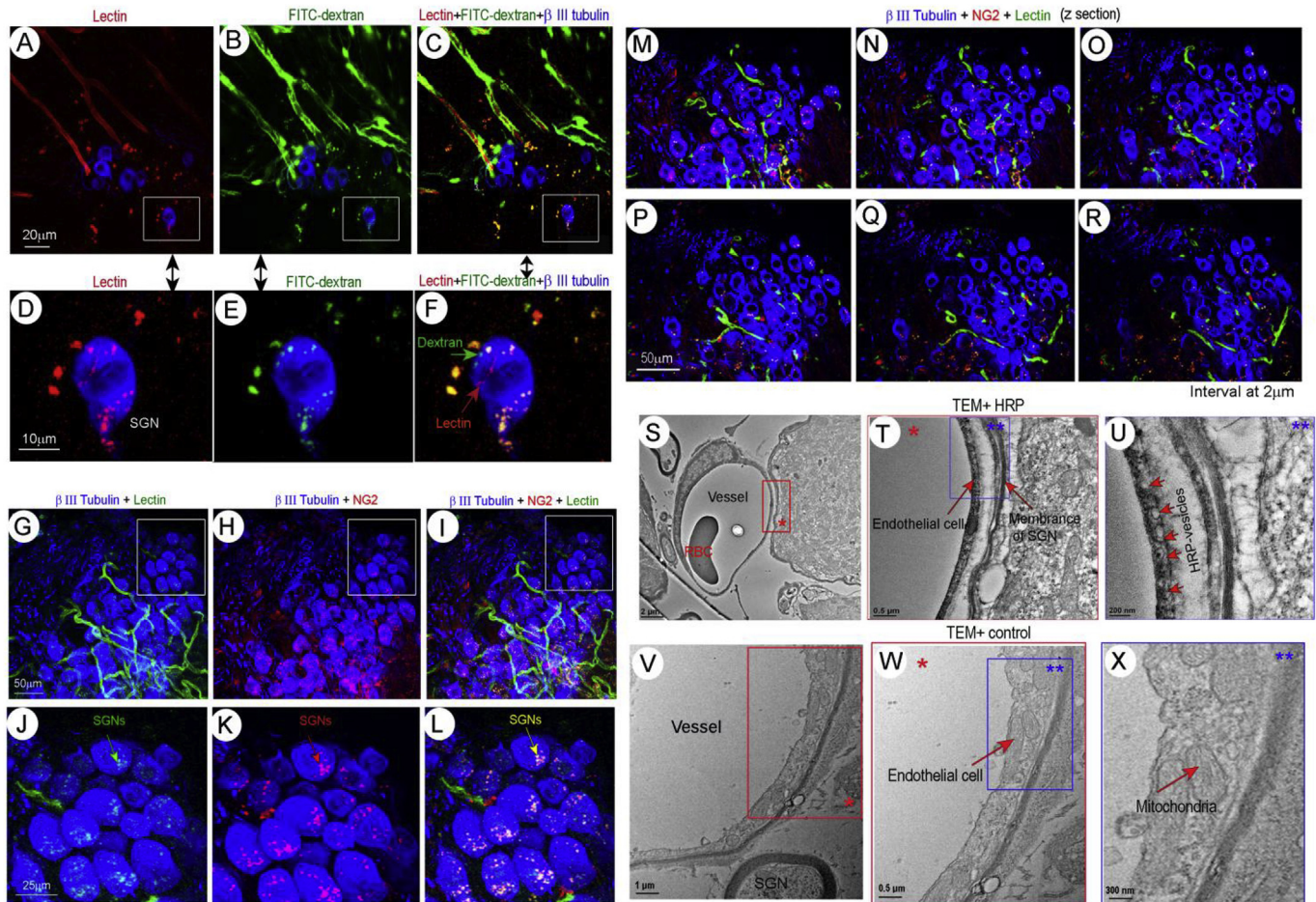


Fig. 7. Cross-talk between SGNs and blood circulation. (A–C) Low magnification confocal projection images show FITC-dextran extravasated from lectin-stained (red) blood vessels taken up by SGNs. (D–F) Close-up images from regions of panels A–C show a neuron labeled with β -III Tubulin having taken up lectin (red, D) and FITC-dextran (green, E). (F) Merger of panels D and E (red arrow points out the lectin signal, green arrow the dextran signal). (G–I) Neurons labeled with β -III Tubulin also take up lectin (green, G) and NG2 particles (red, H), shown under low magnification. (I) Merger of panels G and H. (J–L) Close-up images from regions of panels G–I show respective cellular fluorescence signals of lectin (green), NG2 (red), and green/NG2 (yellow). (M–R) Confocal z-section images at 2 μ m intervals further show the lectin and NG2 signals in the soma of SGNs. (S–U) TEM images from the HRP treated group show capillaries under low (S) and high magnification (T) from insert (*) in pane (S). The capillaries situate at a distance from neurons, with no clear physical contact between them. (U) A high magnification TEM micrograph from insert (**) in panel K shows multiple HRP containing vesicles in the ECs. (V and W) TEM images from the control group show a capillary wall under low (V) and high magnification (W) from insert * in panel (V). (X) A high magnification TEM micrograph from insert (**) in panel W shows cellular organelles, such as mitochondria, in the EC, but no obvious HRP-vesicles in the EC. PP: peripheral processes; RBC: red blood cell; HRP: horseradish peroxidase. (For interpretation of the references to colour in this figure legend, the reader is referred to the Web version of this article.)

Montagne et al., 2018; Wang et al., 2014).

In addition, recent studies have revealed that pericytes release growth factors such as basic fibroblast growth factor, hepatocyte growth factor, epidermal growth factor, and angiopoietin (Chen et al., 2013; Gaceb et al., 2018; Katare et al., 2011). In this study, we found NG⁺ positive particles taken up by SGNs. This indicates intercellular communication between SGNs and pericytes. The communication may be important for maintenance of neurons, which benefit from the growth factors provided by surrounding pericytes. However, further study is needed to test the hypothesis and identify the full extent of the role of pericytes in this region.

4.3. Interactions between vascular cells and spiral ganglion neurons

In the brain, we see a neurovascular unit (BBB), composed of neurons, astrocytes, endothelial cells, pericytes, and extracellular matrix (Baeten and Akassoglou, 2011; Gautam et al., 2016). These cells, through their intimate anatomical and chemical relationship, detect neuronal need and trigger vasodilation or vasoconstriction to accommodate the neuron demand (Iadecola, 2017). How does

the vascular system meet the SGN demand and sustain hearing activity? Large vessels in the region of SGNs are richly innervated by nerve fibers from the peripheral autonomic and sensory ganglion, including the superior cervical, sphenopalatine, and trigeminal ganglion, controlling blood flow in response to neuron activity (Hamel, 2006; Vass et al., 1998). The smallest vessels, the capillaries, provide for direct metabolite exchange and act as the primary barrier between blood and surrounding tissue. Whether neuro-vascular coupling at the capillary level, such as seen in the brain, helps accommodate the energy demand of SGNs is an open question. In this study, we investigated possible structural links between the vascular and neural system using a double transgenic fluorescent reporter mouse in combination with immunofluorescence labeling and TEM. Our data did not support direct physical coupling of neuron signaling to capillaries via bridge cells analogous to astrocytes in the brain. Under confocal fluorescence microscopy, we found some capillaries to palisade along acoustic nerve fibers but we could not corroborate under TEM any direct contacts between capillaries and satellite cells (major glial cells surrounding the soma of spiral ganglion neurons). Under TEM,

capillary vessels were “isolated” from surrounding tissue, with no obvious direct contacts. However, fluorescent substrates (FITC-dextran) injected into the blood circulation are taken up by neurons. In particular, after injection of HRP tracer, we clearly observed under TEM accumulation of HRP in the adjoining extracellular spaces, with the endothelial wall showing membranous inclusions of the HRP and in endothelial cells multiple vesicles. This is indicative of transport activity between the vessels and extracellular space. Most interestingly, we found neurons not only take up substances from the blood, but also take up secreted substances from vascular pericytes, as shown in Fig. 7. We conclude there is active exchange between the two systems, although the exact mechanism of transport between the two systems needs further study.

In summary, visualization of the vasculature in the spiral ganglion and peripheral processes is markedly improved under a tissue clearing protocol. A relatively dense vascular network is seen in young adult mice, which thins out as the animals age, particularly in the SL. Tissue resident macrophages surrounding the blood vessels undergo drastic changes in morphology from young animal (P7) to adult (P30). The pericytes densely populating vascular networks display some heterogeneity. Conspicuous endocytotic transport is observed between spiral ganglion nerves and the vascular system.

Conflict of interest disclosure statement

All authors have read and approved the manuscript, and none have a financial or personal interest which presents a conflict of interest with its content.

Acknowledgments

This project was conducted at Oregon Hearing Research Center, Department of Otolaryngology and Head and Neck Surgery, Oregon Health and Science University. The work was supported by the National Institutes of Health grants NIH/NIDCD R21 DC016157 (X. Shi), NIH/NIDCD R01 DC015781 (X. Shi), NIH P30-DC005983 (Peter Barr-Gillespie), and Medical Research Foundation from Oregon Health and Science University MRF (X. Shi).

Appendix A. Supplementary data

Supplementary data to this article can be found online at <https://doi.org/10.1016/j.heares.2018.11.012>.

References

- Aguilera, K.Y., Brekken, R.A., 2014. Recruitment and retention: factors that affect pericyte migration. *Cell. Mol. Life Sci.* 71, 299–309.
- Andreone, B.J., Lacoste, B., Gu, C., 2015. Neuronal and vascular interactions. *Annu. Rev. Neurosci.* 38, 25–46.
- Angelborg, C., Axelsson, A., Larsen, H.C., 1984. Regional blood flow in the rabbit cochlea. *Arch. Otolaryngol.* 110, 297–300.
- Armulik, A., Genove, G., Mae, M., Nisancioglu, M.H., Wallgard, E., Niaudet, C., He, L., Norlin, J., Lindblom, P., Strittmatter, K., Johansson, B.R., Betsholtz, C., 2010. Pericytes regulate the blood-brain barrier. *Nature* 468, 557–561.
- Axelsson, A., 1988. Comparative anatomy of cochlear blood vessels. *Acta Otolaryngol.* 9, 278–290.
- Baeten, K.M., Akassoglou, K., 2011. Extracellular matrix and matrix receptors in blood-brain barrier formation and stroke. *Dev Neurobiol* 71, 1018–1039.
- Bao, J., Ohlemiller, K.K., 2010. Age-related loss of spiral ganglion neurons. *Hear. Res.* 264, 93–97.
- Bas, E., Goncalves, S., Adams, M., Dinh, C.T., Bas, J.M., Van De Water, T.R., Eshraghi, A.A., 2015. Spiral ganglion cells and macrophages initiate neuroinflammation and scarring following cochlear implantation. *Front. Cell. Neurosci.* 9, 303.
- Block, M.L., Hong, J.S., 2005. Microglia and inflammation-mediated neurodegeneration: multiple triggers with a common mechanism. *Prog. Neurobiol.* 76, 77–98.
- Block, M.L., Zecca, L., Hong, J.S., 2007. Microglia-mediated neurotoxicity: uncovering the molecular mechanisms. *Nat. Rev. Neurosci.* 8, 57–69.
- Brown, L.N., Xing, Y., Noble, K.V., Barth, J.L., Panganiban, C.H., Smythe, N.M., Bridges, M.C., Zhu, J., Lang, H., 2017. Macrophage-mediated glial cell elimination in the postnatal mouse cochlea. *Front. Mol. Neurosci.* 10, 407.
- Chen, C.W., Okada, M., Proto, J.D., Gao, X., Sekiya, N., Beckman, S.A., Corselli, M., Crisan, M., Saparov, A., Tobita, K., Peault, B., Huard, J., 2013. Human pericytes for ischemic heart repair. *Stem Cell.* 31, 305–316.
- Cheret, C., Gervais, A., Lelli, A., Colin, C., Amar, L., Ravassard, P., Mallet, J., Cumano, A., Krause, K.H., Mallat, M., 2008. Neurotoxic activation of microglia is promoted by a nox1-dependent NADPH oxidase. *J. Neurosci.* 28, 12039–12051.
- Chung, K., Wallace, J., Kim, S.Y., Kalyanasundaram, S., Andelman, A.S., Davidson, T.J., Mirzabekov, J.J., Zolocsky, K.A., Mattis, J., Denisin, A.K., Pak, S., Bernstein, H., Ramakrishnan, C., Grosenick, L., Gradinaru, V., Deisseroth, K., 2013. Structural and molecular interrogation of intact biological systems. *Nature* 497, 332–337.
- Crawford, C., Wildman, S.S., Kelly, M.C., Kennedy-Lydon, T.M., Peppatt-Wildman, C.M., 2013. Sympathetic nerve-derived ATP regulates renal medullary vasa recta diameter via pericyte cells: a role for regulating medullary blood flow? *Front. Physiol.* 4, 307.
- Daneman, R., Zhou, L., Kebede, A.A., Barres, B.A., 2010. Pericytes are required for blood-brain barrier integrity during embryogenesis. *Nature* 468, 562–566.
- De Silva, T.M., Miller, A.A., 2016. Cerebral small vessel disease: targeting oxidative stress as a novel therapeutic strategy? *Front. Pharmacol.* 7, 61.
- Dias Moura Prazeres, P.H., Sena, I.F.G., Borges, I.D.T., de Azevedo, P.O., Andreotti, J.P., de Paiva, A.E., de Almeida, V.M., de Paula Guerra, D.A., Pinheiro Dos Santos, G.S., Mintz, A., Delbono, O., Birbrair, A., 2017. Pericytes are heterogeneous in their origin within the same tissue. *Dev. Biol.* 427, 6–11.
- Dong, Y., Zhang, C., Frye, M., Yang, W., Ding, D., Sharma, A., Guo, W., Hu, B.H., 2018. Differential fates of tissue macrophages in the cochlea during postnatal development. *Hear. Res.* 365, 110–126.
- Doshi, N., Mitragotri, S., 2010. Macrophages recognize size and shape of their targets. *PLoS One* 5, e10051.
- Ellis, C.G., Jagger, J., Sharpe, M., 2005. The microcirculation as a functional system. *Crit. Care* 9 (Suppl. 4), S3–S8.
- Firbas, W., Gruber, H., Wicke, W., 1981. The blood vessels of the limbus spiralis. *Arch. Oto-Rhino-Laryngol.* 232, 131–137.
- Folkman, J., Moscona, A., 1978. Role of cell shape in growth control. *Nature* 273, 345–349.
- Gaceb, A., Ozen, I., Padel, T., Barbariga, M., Paul, G., 2018. Pericytes secrete pro-regenerative molecules in response to platelet-derived growth factor-BB. *J. Cerebr. Blood Flow Metabol.* 38, 45–57.
- Gautam, J., Zhang, X., Yao, Y., 2016. The role of pericytic laminin in blood brain barrier integrity maintenance. *Sci. Rep.* 6, 36450.
- Gyo, K., 2013. Experimental study of transient cochlear ischemia as a cause of sudden deafness. *World J. Otorhinolaryngol.* 3 (1), 1–15.
- Hamel, E., 2006. Perivascular nerves and the regulation of cerebrovascular tone. *J. Appl. Physiol.* 100, 1059–1064, 1985.
- Hanisch, U.K., Kettenmann, H., 2007. Microglia: active sensor and versatile effector cells in the normal and pathologic brain. *Nat. Neurosci.* 10, 1387–1394.
- Hellstrom, M., Kalen, M., Lindahl, P., Abramsson, A., Betsholtz, C., 1999. Role of PDGF-B and PDGF-beta in recruitment of vascular smooth muscle cells and pericytes during embryonic blood vessel formation in the mouse. *Development* 126, 3047–3055.
- Hirschi, K.K., D’Amore, P.A., 1996. Pericytes in the microvasculature. *Cardiovasc. Res.* 32, 687–698.
- Iadecola, C., 2017. The neurovascular unit coming of age: a journey through neurovascular coupling in health and disease. *Neuron* 96, 17–42.
- Jing, D., Zhang, S., Luo, W., Gao, X., Men, Y., Ma, C., Liu, X., Yi, Y., Bugde, A., Zhou, B.O., Zhao, Z., Yuan, Q., Feng, J.Q., Gao, L., Ge, W.P., Zhao, H., 2018. Tissue clearing of both hard and soft tissue organs with the PEGASOS method. *Cell Res.* 28, 803–818.
- Katare, R., Riu, F., Mitchell, K., Gubernator, M., Campagnolo, P., Cui, Y., Fortunato, O., Avolio, E., Cesselli, D., Beltrami, A.P., Angelini, G., Emanueli, C., Madeddu, P., 2011. Transplantation of human pericyte progenitor cells improves the repair of infarcted heart through activation of an angiogenic program involving microRNA-132. *Circ. Res.* 109, 894–906.
- Kaur, T., Ohlemiller, K.K., Warchol, M.E., 2018. Genetic disruption of fractalkine signaling leads to enhanced loss of cochlear afferents following ototoxic or acoustic injury. *J. Comp. Neurol.* 526, 824–835.
- Kaur, T., Zamani, D., Tong, L., Rubel, E.W., Ohlemiller, K.K., Hirose, K., Warchol, M.E., 2015. Fractalkine signaling regulates macrophage recruitment into the cochlea and promotes the survival of spiral ganglion neurons after selective hair cell lesion. *J. Neurosci.* 35, 15050–15061.
- Kisler, K., Nelson, A.R., Montagne, A., Zlokovic, B.V., 2017. Cerebral blood flow regulation and neurovascular dysfunction in Alzheimer disease. *Nat. Rev. Neurosci.* 18, 419–434.
- Kujawa, S.G., Liberman, M.C., 2015. Synaptopathy in the noise-exposed and aging cochlea: primary neural degeneration in acquired sensorineural hearing loss. *Hear. Res.* 330, 191–199.
- Lindahl, P., Hellstrom, M., Kalen, M., Betsholtz, C., 1998. Endothelial-perivascular cell signaling in vascular development: lessons from knockout mice. *Curr. Opin. Lipidol.* 9, 407–411.
- MacDonald, G.H., Rubel, E.W., 2008. Three-dimensional imaging of the intact mouse cochlea by fluorescent laser scanning confocal microscopy. *Hear. Res.* 243, 1–10.
- Mitrasinovic, O.M., Murphy Jr., G.M., 2002. Accelerated phagocytosis of amyloid-

- beta by mouse and human microglia overexpressing the macrophage colony-stimulating factor receptor. *J. Biol. Chem.* 277, 29889–29896.
- Mirrasinovic, O.M., Grattan, A., Robinson, C.C., Lapusnea, N.B., Poon, C., Ryan, H., Phong, C., Murphy Jr., G.M., 2005. Microglia overexpressing the macrophage colony-stimulating factor receptor are neuroprotective in a microglial-hippocampal organotypic coculture system. *J. Neurosci.* 25, 4442–4451.
- Montagne, A., Nikolakopoulou, A.M., Zhao, Z., Sagare, A.P., Si, G., Lazic, D., Barnes, S.R., Daianu, M., Ramanathan, A., Go, A., Lawson, E.J., Wang, Y., Mack, W.J., Thompson, P.M., Schneider, J.A., Varkey, J., Langen, R., Mullins, E., Jacobs, R.E., Zlokovic, B.V., 2018. Pericyte degeneration causes white matter dysfunction in the mouse central nervous system. *Nat. Med.* 24, 326–337.
- Nakashima, T., Suzuki, T., Iwagaki, T., Hibi, T., 2001. Effects of anterior inferior cerebellar artery occlusion on cochlear blood flow—a comparison between laser-Doppler and microsphere methods. *Hear. Res.* 162, 85–90.
- Neng, L., Zhang, F., Kachelmeier, A., Shi, X., 2013. Endothelial cell, pericyte, and perivascular resident macrophage-type melanocyte interactions regulate cochlear intrastriatal fluid-blood barrier permeability. *J Assoc Res Otolaryngol* 14, 175–185.
- Neng, L., Zhang, J., Yang, J., Zhang, F., Lopez, I.A., Dong, M., Shi, X., 2015. Structural changes in the stria vascularis blood-labyrinth barrier of aged C57BL/6 mice. *Cell Tissue Res.* 361, 685–696.
- Nimmerjahn, A., Kirchhoff, F., Helmchen, F., 2005. Resting microglial cells are highly dynamic surveillants of brain parenchyma in vivo. *Science* 308, 1314–1318.
- Noonan, J.E., Lamoureux, E.L., Sarossy, M., 2015. Neuronal activity-dependent regulation of retinal blood flow. *Clin. Exp. Ophthalmol.* 43, 673–682.
- Okano, T., Nakagawa, T., Kita, T., Kada, S., Yoshimoto, M., Nakahata, T., Ito, J., 2008. Bone marrow-derived cells expressing Iba1 are constitutively present as resident tissue macrophages in the mouse cochlea. *J. Neurosci. Res.* 86, 1758–1767.
- Ostergaard, L., Engedal, T.S., Moreton, F., Hansen, M.B., Wardlaw, J.M., Dalkara, T., Markus, H.S., Muir, K.W., 2016. Cerebral small vessel disease: capillary pathways to stroke and cognitive decline. *J. Cerebr. Blood Flow Metabol.* 36, 302–325.
- Pacilli, A., Pasquinelli, G., 2009. Vascular wall resident progenitor cells: a review. *Exp. Cell Res.* 315, 901–914.
- Peppiatt, C.M., Howarth, C., Mobbs, P., Attwell, D., 2006. Bidirectional control of CNS capillary diameter by pericytes. *Nature* 443, 700–704.
- Richardson, D.S., Lichtman, J.W., 2015. Clarifying tissue clearing. *Cell* 162, 246–257.
- Shapouri-Moghaddam, A., Mohammadian, S., Vazini, H., Taghadosi, M., Esmaeili, S.A., Mardani, F., Seifi, B., Mohammadi, A., Afshari, J.T., Sahebkar, A., 2018. Macrophage plasticity, polarization, and function in health and disease. *J. Cell. Physiol.* 233, 6425–6440.
- Shi, X., 2016. Pathophysiology of the cochlear intrastriatal fluid-blood barrier (review). *Hear. Res.* 338, 52–63.
- Shi, X., Han, W., Yamamoto, H., Tang, W., Lin, X., Xiu, R., Trune, D.R., Nuttall, A.L., 2008. The cochlear pericytes. *Microcirculation* 15, 515–529.
- Sims, D.E., 2000. Diversity within pericytes. *Clin. Exp. Pharmacol. Physiol.* 27, 842–846.
- Vacca, A., Ribatti, D., 2011. Angiogenesis and vasculogenesis in multiple myeloma: role of inflammatory cells. Recent results in cancer research. *Fortschritte der Krebsforschung. Progrès dans les recherches sur le cancer* 183, 87–95.
- Vass, Z., Shore, S.E., Nuttall, A.L., Miller, J.M., 1998. Direct evidence of trigeminal innervation of the cochlear blood vessels. *Neuroscience* 84, 559–567.
- Venkat, P., Chopp, M., Chen, J., 2016. New insights into coupling and uncoupling of cerebral blood flow and metabolism in the brain. *Croat. Med. J.* 57, 223–228.
- Wang, Y., Pan, L., Moens, C.B., Appel, B., 2014. Notch3 establishes brain vascular integrity by regulating pericyte number. *Development* 141, 307–317.
- Wilhelm, K., Happel, K., Eelen, G., Schoors, S., Oellerich, M.F., Lim, R., Zimmermann, B., Aspalter, I.M., Franco, C.A., Boettger, T., Braun, T., Fruttiger, M., Rajewsky, K., Keller, C., Bruning, J.C., Gerhardt, H., Carmeliet, P., Potente, M., 2016. FOXO1 couples metabolic activity and growth state in the vascular endothelium. *Nature* 529, 216–220.
- Yagihashi, A., Sekiya, T., Suzuki, S., 2005. Macrophage colony stimulating factor (M-CSF) protects spiral ganglion neurons following auditory nerve injury: morphological and functional evidence. *Exp. Neurol.* 192, 167–177.
- Zengin, E., Chalajour, F., Gehling, U.M., Ito, W.D., Treede, H., Lauke, H., Weil, J., Reichenhals, H., Kilic, N., Ergun, S., 2006. Vascular wall resident progenitor cells: a source for postnatal vasculogenesis. *Development* 133, 1543–1551.